RSC Mechanochemistry

ROYAL SOCIETY OF CHEMISTRY

PAPER

View Article Online
View Journal | View Issue

Cite this: *RSC Mechanochem.*, 2025, **2**, 911

Experimental quantification of impact force and energy for mechanical activation in vibratory ball mills

Emmanuel Nwoye, [a] Kathleen Floyd, [b] James Batteas *[b] and Jonathan Felts *[a]

Mechanochemistry has been shown to provide a greener alternative to chemical synthesis; however, challenges in establishing clear relationships between chemical reaction yields and operational reactor parameters, such as milling frequency, milling ball material properties, vessel material properties, and reactor geometries used in a mechanochemical synthesis, make optimizing reactor efficiency difficult. This study presents a force model that relates these reactor parameters to quantifiable impact forces within a vibratory ball mill. To validate this force model, we developed a method for integrated, real-time measurement of force ensembles in the reaction vessel by embedding piezoresistive sensors with fast response to capture impact dynamics at various milling frequencies and operational settings. We measured force using preground NaCl at different fill ratios and compared it to an adjusted Hertzian contact mechanics force model with fill factor. We found agreement between the measured and modeled impact force. At the macroscale, impact acts as an ensemble of forces dynamically applied to the reactants. By simulating the mechanical activation of an illustrative mechanochemical system with known energetics, we show that there is little to no difference in effect between using the mean impact force and force ensemble on the kinetics of a straightforward mechanochemical reaction. We also demonstrate kinetic energy quantification in the Knoevenagel condensation reaction of vanillin and barbituric acid to understand what fraction of kinetic energy goes toward mechanical activation. We observed that the energetics of high-frequency milling for this reaction system entail diminishing returns, reinforcing the notion that there can be an optimal balance between collision intensity, resulting impact forces, and productive energy usage. The developed toolset and models provide a framework for understanding mechanochemical activation in vibratory ball mills and optimizing reaction parameters for scale-up to other reactors.

Received 30th April 2025
Accepted 27th August 2025

DOI: 10.1039/d5mr00059a

rsc.li/RSCMechanochem

1. Introduction

Mechanochemistry offers energy-efficient and solvent-free alternatives for chemical synthesis. It utilizes mechanical energy to achieve chemical transformations in solid-state reactant systems.[1–3] Understanding the underlying mechanisms of mechanochemical reactions begins with a firm grasp of how reactors facilitate mechanical activation and subsequent stress relaxations in reactive solids.[4,5] Examples of these reactors include mortars and pestles, ball mills, twin screw extruders, and resonant acoustic mixers.[6,7] Ball milling is a particularly important and common reactor system for mechanochemical synthesis, involving grinding solid particles through continuous deformation and fracturing using hard milling media.[8,9] Ball mills come in various types, each suited for a specific application and scale. Vibratory ball mills use high-energy vibration and repeated excitation to agitate a milling enclosure containing milling media and the material being milled. These vibrations cause the milling media to impact the reactants, thus facilitating particle size reduction and subsequent chemical transformation. Other milling methods, such as planetary ball mills, use the effect of gravity and rotational motions to create centrifugal forces for grinding. Attrition mills, suited for wet and dry grinding, use vertical and horizontal rotating shafts with arms to stir grinding media and materials.[10,11]

Insights into how these instruments influence reactivity, and specifically how applied force affects reaction kinetics, have become increasingly important.[12] As a result, the study of impact dynamics in ball mills has garnered significant interest due to its pivotal role in understanding and optimizing mechanochemical reactions. Researchers have extensively studied the effects of ball mill material, frequency, vessel loading, and

[a]*Advanced Nanomanufacturing Laboratory, Department of Mechanical Engineering, Texas A&M University, College Station, Texas-77843-3123, USA. E-mail: jonathan.felts@tamu.edu*

[b]*Department of Chemistry, Texas A&M University, College Station, TX 77842, USA*

milling media sizes to elucidate the parameters that affect reactivity and selectivity.[13–15] However, the literature presents diverse findings that are often conflicting regarding the dynamics and magnitude of impact forces involved and the optimal conditions for mechanochemical reactions. Studies have shown that the complex ball dynamics in vibratory ball mills involve macroscopic (system-level) and microscopic (collision-level) interactions.[16–22] At the macroscopic level, the overall motion of the ball and vial significantly influences the milling process and exhibits periodic and chaotic behaviour. Predictable ball/vial motion patterns characterize the periodic mode, where each collision provides a uniform energy input, and irregular ball motion characterizes the chaotic mode. At the microscopic level, the effects of impact, shear, and friction forces highlight the interactions between reactant particles and the milling ball.

Efforts in mechanochemistry have focused on phenomenological kinetic models that describe the complex nature of ball-milling reactions using the input reaction parameters. For example, one model for highly deformable molecular solids incorporates the statistical nature of ball milling by considering how the mass of reactant powder trapped during a collision is remixed with unreacted powder at the end of the event.[23] This framework relates experimental kinetic curves to the deformation experienced during impacts by integrating reaction parameters such as interface generation, reaction probability, and powder volume processed during an individual impact. Other kinetic models, which consider factors such as energy dose, have highlighted how key milling parameters, including collision energy and frequency, influence reactivity.[24,25] Although mid-20th-century studies exhaustively mapped ball-mill kinematics, the actual forces that activate powder during each collision event remain experimentally unresolved. Studies by Avvakumov *et al.*, along with Urakaev's models, transformed ball trajectories into semi-quantitative maps of impact velocity and energy input.[26,27] The coupled momentum transfer and kinetic models developed by Smolyakov *et al.*, along with the nomograms proposed by Yusupov *et al.*, continue to inform device comparisons today.[28,29] Butyagin *et al.* introduced the energy-yield concept, which highlights that only a fraction of the mechanical work applied to the jar is stored as defects that drive reactions, a point recently supported by Rogachev's study of heterogeneous collision.[30–32] However, all these benchmarks rely on indirect proxies, such as detachment radii, indent sizes, vial temperatures, and DEM models, to estimate force amplitudes.

Mechanistic approaches involve quantifying the deformation caused by impact forces during the milling process. These deformations include structural changes to the milling media and vessel, as well as elastic and plastic deformations of the reactant powder.[33] Elastic deformation is important because it allows reversible energy storage, whereas plastic deformation causes lattice defects, amorphization, and surface activation—factors that enhance mechanochemical reactivity. Simultaneously, excessive deformation of the milling media can lead to energy loss, unproductive work, and potential contamination. Therefore, understanding these deformation processes precisely is vital for identifying thresholds that optimize impact forces and improve milling efficiency. The Hertz contact model has long been effective in describing such deformations, especially in low-energy, elastic collision regimes. However, for high-speed systems with velocities exceeding 10 m s^{-1}, the limitations of the Hertz model become apparent.[34]

Accurately measuring impact force in these ball milling systems is challenging, as it requires the strategic placement of force sensors to capture impact effectively. An inverse technique, where impact forces were predicted from acceleration measurements, yielded quantities on the order of hundreds of newtons, suggesting that this range of forces is necessary to induce mechanochemical reactions.[20] However, subsequent studies have indicated that increasing milling frequencies and amplitudes generally increase impact forces to the order of thousands of newtons, enhancing the milling process through more effective deformation, welding, and fracture of powder particles.[20,35,36] One study utilized the Kelvin dashpot-spring model and discrete element method simulations to examine milling ball motion within a vibratory ball mill. The results revealed significantly lower milling ball velocities when benchmarked against prior studies operating at similar milling frequencies, implying even lower impact forces.[37] These discrepancies between model predictions and earlier experimental measurements highlight the complexities of capturing the impact forces within vibratory ball mills.

Despite the recognition that mechanical energy is the primary driving force of solid-state reactivity, precise quantification of how that energy is delivered during each collision remains elusive.[4,5] Recent efforts to standardize disparate milling platforms by normalizing the dose of kinetic energy supplied to the powder highlight how reactor geometry significantly obscures direct comparisons of published kinetics.[38] Weidenthaler *et al.* demonstrated that the overall energy required to complete an alkali-halide metathesis is invariant with milling frequency and that periodic pressure pulses, rather than bulk heating, are the dominant driving force.[39] Complementary studies by Delogu, Carta *et al.* mapped individual impact events to global transformation curves and revealed that only a subset of collisions reach the stress threshold needed for chemical change; however, they could not resolve the force profile within each event.[40] Takacs' kinetic analyses further demonstrated (i) a minimum impact energy of a few hundred millijoules below which no reaction proceeds, and (ii) that just micrograms of powder are processed per collision, yet these insights relied on indirect metrics such as ignition time or statistical modelling.[41,42] Very recently, contact mechanics studies have cautioned that neglecting spatially non-uniform stress can lead to misestimation of activation volumes by orders of magnitude, underscoring the need for direct force measurements.[43]

Here, we address this challenge by embedding piezoresistive sensors into a vibratory milling jar, capturing the full force ensemble in real-time as shown in Fig. 1 and validating a fill-ratio-corrected Hertz model against these measurements. We then used pre-ground NaCl as the reactant mixture to extract the impact force reduction factor as the reactant fill ratio varies. We

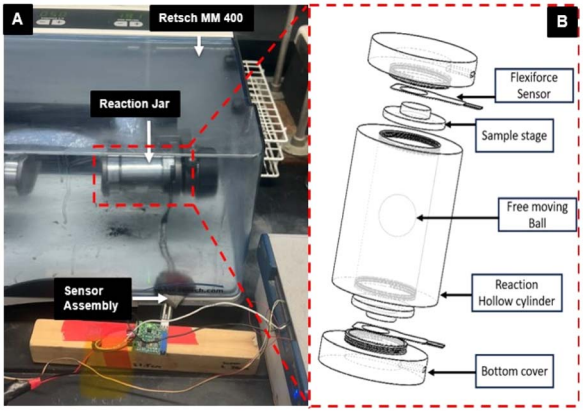

Fig. 1 Schematic of integrated reaction jar. (A) Reactor jar with integrated force measurement in the Retsch MM400. (B) 3D model of the assembled jar featuring the force sensing assembly.

utilize a previously established kinetic framework to simulate an illustrative mechanochemical system with known energetics, thereby quantifying how the observed force ensembles in vibratory ball mills influence the overall kinetics.[44] Lastly, by using this force-sensing vessel in a Retsch MM400 vibratory ball mill, which can achieve both fine and ultrafine grinding, we experimentally estimate the kinetic energy transferred to reactant particles in the Knoevenagel condensation of vanillin and barbituric acid.

2. Theory of force-driven chemistry in a vibratory ball mill

Consider a reciprocating ball mill that translates a distance L with a frequency of f. We further assume that, on average, the ball within the mill has a speed of zero relative to the global frame of reference and a speed $v = 2fL$ with respect to the reciprocating mill. The ball then impacts the vessel's side with energy $K = 0.5mv^2$ where m is the ball's mass and v is the ball's speed. Some fraction of the energy φ transfers from the ball to the vessel wall. Under the assumption of elastic collisions, the impact force can be related to the transfer of energy using Hertz contact mechanics between a sphere and a half-space.

$$K = Fd \tag{1}$$

where F is the force and d is the indentation depth.

$$d = \left(\frac{9}{16}\right)^{1/3}\left(\frac{F^2}{E^{*2}R}\right)^{1/3} \tag{2}$$

Using the elastic modulus, E and Poisson ratio, ϖ for the ball and vessel materials, the effective mechanical modulus E^* is given by

$$E^* = \left[\frac{1-\varpi_1}{E_1} + \frac{1-\varpi_2}{E_2}\right]^{-1}. \tag{3}$$

The radius of impact is expressed in terms of the radius of the ball R_b and the radius of the reaction vessel curved ends R_c

$$R = \left(\frac{1}{R_b} - \frac{1}{R_c}\right)^{-1}. \tag{4}$$

Applying (2) to (1), and rearranging, gives

$$F = \left[\frac{KE^{*2/3}R^{1/3}}{\left(\frac{9}{16}\right)^{5/6}}\right]^{3/5}. \tag{5}$$

Force is then described in terms of geometric and material properties as

$$F = 1.75\left[E^*\left(\rho {R_b}^3(2lf)^2\right)^{\frac{3}{2}}R^{\frac{1}{2}}\right]^{2/5}, \tag{6}$$

where ρ is the density of the ball. Eqn (6) shows that the force depends on the density of the milling media, the geometry of the ball and vessel, the collision frequency, the travel length of the ball, and the material strength. Next, we incorporate reactant fill ratio into the force model to understand how it affects the impact force. We defined the fill ratio V_r as

$$V_r = \frac{V_b + V_c}{V_v}, \tag{7}$$

where V_b is the volume of milling media (ball), V_c is the volume of reactants and V_v is the volume of the reaction vessel. The reduction factor, which defines how the impact force reduces with the fill ratio, is determined from experimental measurements, as shown in the SI.

To quantify what fraction of milling ball energy goes towards mechanical activation, the total kinetic energy K_0 imparted from the milling ball to the reaction is taken as a summation of several components:

- The energy used to alter the potential energy surfaces (PES), overcome the energy barrier, and reach a transition state, thus facilitating reactivity (K_{act}).
- The kinetic energy that enables defects and fracturing of particles to generate smaller particle sizes, thus creating new surfaces that enhance diffusion and reactivity (K_d).
- The energy lost due to friction between the reactant mixture, ball, and vessel wall (K_{fr}).
- The energy absorbed by the vessel wall through plastic and elastic deformation (K_v).
- The residual kinetic energy retained by particles after impact (K_p).

The total kinetic balance is expressed in eqn (8) as

$$K_0 = K_{act} + K_d + K_{fr} + K_v + K_p \tag{8}$$

Here,

$$K_0 = \frac{1}{2}m_b{v_b}^2 = F \times d_i \tag{9}$$

where m_b is the mass of the milling ball, v_b is the velocity of milling balls, F is the force exerted by the milling ball and d_i is the deformation. Therefore, the total kinetic energy K_0 can be expressed as

$$K_0 = F_{en}\Delta x + \gamma_s \Delta A + \sum_i F_{fr,i}\Delta s_i + \sum_i \left(\frac{1}{2} m_{p,i} {v_{p,i}}^2\right) + K_v, \quad (10)$$

where F_{en} is the force ensemble acting on the reactants, Δx is the effective path length along the reaction coordinate, γ_s is the specific surface energy, and ΔA is the new surface area created due to fracture. The energy loss due to friction is the summation of the frictional force F_{fr} over sliding distance Δs for all particles. Residual particle energy is the summation of all particles i within the contact, where m_p is the mass of the reactant particles and v_p is the velocity of particles. The energy absorbed by the vessel K_v is estimated by measuring the force transmitted to the vessel over time.

If the particles are pre-ground, the energy going towards particle fracture is negligible. Further, we assume that the kinetic and frictional parameters of the particles are equal during and after the reaction, and so taking the difference between eqn (10) during and after the reaction is complete leads to a measurement of energy transferred to the reactants

$$K_{act} = K_{v,complete} - K_{v,during}, \quad (11)$$

where $K_{v,complete}$ is the energy expended within the vessel wall during impact after the reaction is completed.

The energy transferred to the reactants for a single impact can be determined by forces on the reactor wall using Hertz contact mechanics

$$K_{act} = \left(\frac{9}{16 E^{*2} R}\right)^{\frac{1}{3}} \left[{F_{complete}}^{5/3} - {F_{during}}^{5/3}\right], \quad (12)$$

where F is measured by the force sensors in the vessel ends during and when the reaction is complete.

To convert from energy per impact to total energy per mol, we multiply the impact energy by the number of impacts per second and integrate it over time

$$K_{act} = \frac{2}{M}\left(\frac{9}{16 E^{*2} R}\right)^{\frac{1}{3}} \int_{t=0}^{\infty} f\left({F_\infty}^{5/3} - {F_t}^{5/3}\right) dt, \quad (13)$$

where M is the mols of the reactants in the vessel.

3. Results and discussion

3.1. Experimental measurement of impact force and energy using the integrated force-sensing reactant vessel

The vibratory ball mill facilitates frequent collisions between the balls, the reactor wall, other balls, and the material being ground, thus resulting in a distribution of forces throughout the ball mill for each operational setting. The Flexiforce sensors (Tekscan A201-100) used in the modified jars are standard piezoresistive sensors designed for various force-sensing applications with a response time of approximately five microseconds. These sensors were calibrated within a modified operating range to capture impact load between 5 and 4000 N reliably. Sensor calibration was done by applying a known load from a calibrated Benchtop Instron 68TM-10 machine, and the output voltage was recorded. Fig. 2A shows the relationship between the load and voltage, which is used to interpret the voltage signals seen in the Flexiforce sensors during impact in the reactor vessel. Fig. 2B shows the force distribution in one second of impact at 30 Hz for a 12.7 mm diameter stainless steel

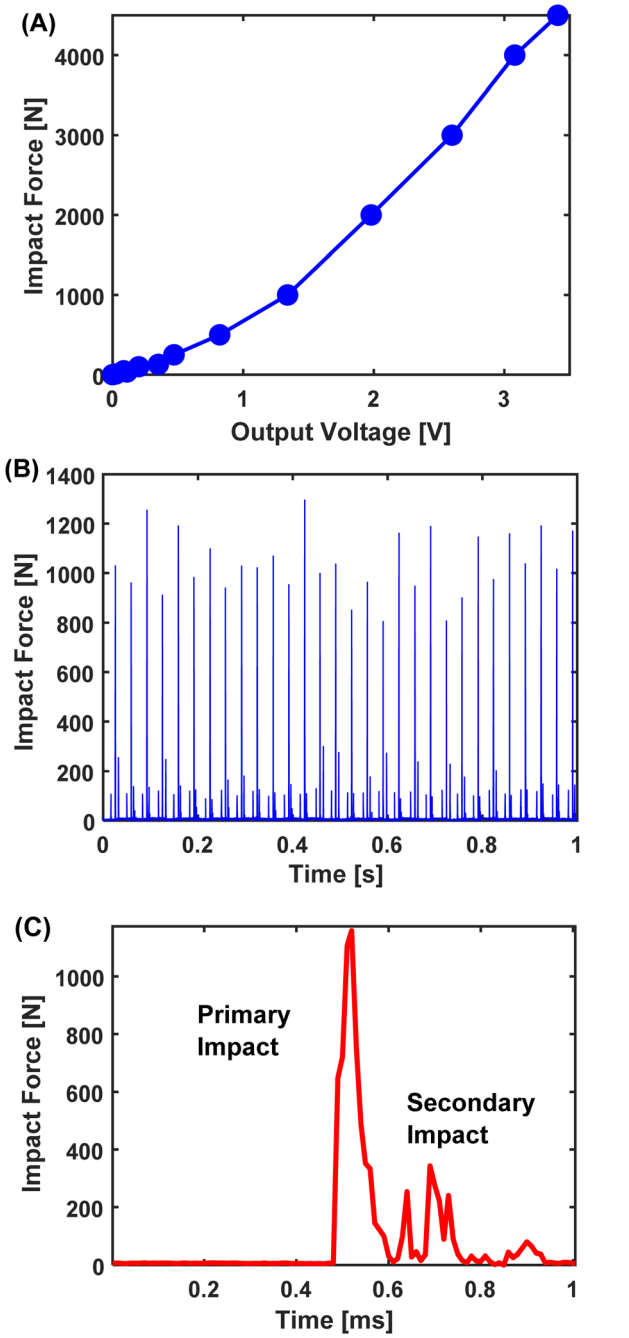

Fig. 2 (A) Flexiforce sensor calibration curve. (B) Representative measurement of impact force using a 12.7 mm SS ball at 30 Hz. (C) Zoomed-in profile of a single impact showing the primary and secondary forces.

ball. The modified reactor vessel had a volume of 14 ml with an end-to-end distance (travel length) of 34 mm. Fig. 2C shows the primary and secondary impact in the ball mill vessel. This real-time force measurement capability is essential to capture detailed information about the force profile in the reaction vessel, especially in mechanochemical systems, where the effect of compressive and shear stresses must be understood. Secondary impacts occur when the milling ball does not directly make contact with the end of the vessel where the sensors are positioned. These impacts result from the chaotic motion of the ball within the milling chamber, leading to indirect force transmission to the sensors. Fig. 3 shows the measured impact force of a milling ball in an empty reaction vessel with integrated force sensors. These force ensembles were measured with varying fill ratios and showed good agreement with the force model described in eqn (6). The Retsch MM400 operates within a milling frequency range of 3 to 30 Hz, with a jar shape (cylindrical with rounded ends), and a motion pattern (linear horizontal oscillation) that directly influences force distribution and energy transfer mechanisms. These parameters notably affect ball trajectories, collision angles, and contact times, which are key factors in determining energy transfer efficiency. Different orientations in vibratory mills may yield distinct ball motion patterns, which will alter the impact ratios observed in this study. Additionally, mills with varying shapes of jars (such as spherical, conical, or custom geometries) will modify ball trajectories and contact areas, necessitating system-specific calibration of force–energy relationships.

Next, we measured how the impact force changes as ball size increases in an empty reaction vessel and compared it with the force model. Here, five ball sizes (ranging between 3.175 mm and 15.875 mm in ball diameter) were used in this impact measurement. Fig. 4 shows the maximum measured impact force compared to the force model for milling balls of various sizes in an empty reaction vessel. The red color represents the modeled impact force, and the blue color represents the measured impact force, with overlap between the measured and modeled impact forces. As shown in Fig. 4, there was a slight difference between the model and force measurement for larger ball *vs.* smaller ball sizes with respect to the diameter of the reaction vessel. This observation agrees with the literature that larger or heavier balls can lead to fewer, less frequent collisions, each with high impulse. In contrast, smaller balls may bounce more erratically with less impulse.[45] Another interesting feature gleaned from the force measurement is capturing the force distribution associated with each parameter. As assumed, the impact in the reactor vessel acts as an ensemble of forces dynamically applied; the force sensors confirm this detail.

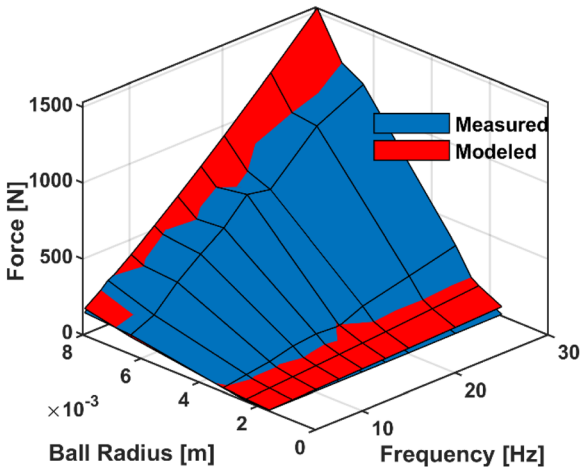

Fig. 4 Maximum measured impact force compared to the force model for empty reaction vessel at different ball sizes and varying milling frequency. The red color represents the modeled impact force, the blue color represents the measured impact force, and the purple color shows the similarity between the measured and modeled impact forces.

Fig. 5 shows the normalized probability density of impact force at various frequencies for a 6.35 mm diameter stainless

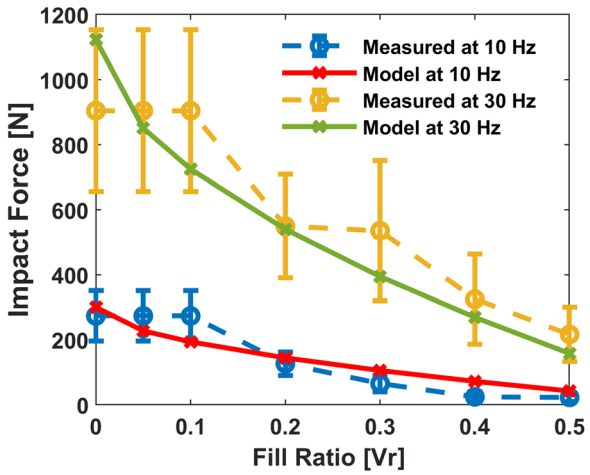

Fig. 3 Impact force measured and modelled as a function of fill ratio for a stainless steel 12.7 mm diameter ball in stainless steel reactor jar at 10 and 30 Hz.

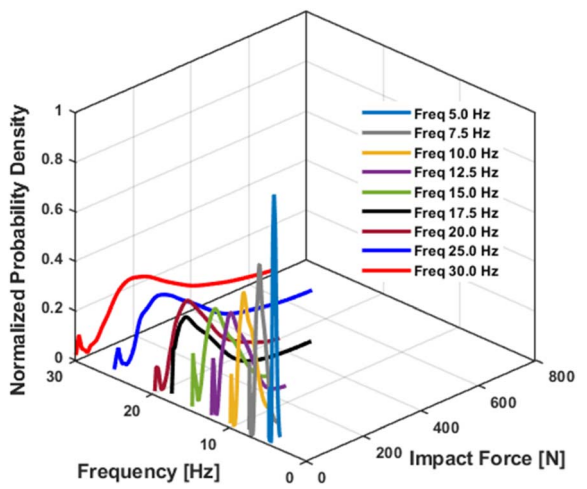

Fig. 5 Impact force ensemble using one 3.15 mm diameter ball in an empty reactor jar for different frequencies.

steel ball in an empty reaction vessel. The secondary impact captured forms a smaller distribution before the primary impact for the entire ball mill frequency range. This effect decreases as frequency increases because there is more ball rolling at lower frequencies due to the ball mill dynamics. At low-frequency impacts, force distribution is tightly clustered around the mean force, which suggests homogeneity in energy transfer from the milling ball to the vessel wall. For a mechanochemical synthesis, this energy transfer homogeneity to the reactant mixture would lead to uniform reaction rates. In high-frequency impact, the impact force varies significantly around the mean force, leading to variability in energy transfer.

Fig. 6A shows the surface plot of how the mean impact force changes with the fill ratio and frequency. Quantifying the forces transmitted from the milling ball to the reactor wall provides insights into how the impact is partitioned between the reactant mixture and the milling assembly. This enables the decoupling of energy contributions from ball–reactant interactions and those dissipated through the vessel, thereby clarifying the extent to which direct impacts drive mechanochemical transformations. Ultimately, accurate force measurements elucidate the effectiveness of energy transfer to the reactants. As shown in Fig. 6A, the measured impact force is significantly reduced from when the reaction vessel is 10 percent filled or less to when the reaction vessel is half-filled for nearly all ball sizes. At low fill levels, there is free space for the ball to accelerate and input energy into the reactant as opposed to when the reaction vessel is half-filled. Fig. 6B shows the kinetic energy going into the reactant particles. Here, at a higher fill ratio, the particles scavenged a more significant portion of the kinetic energy, preventing the ball from impacting the wall of the reactor vessel. At high velocity, heavier and larger balls become oversized, thus leading to frictional losses, energy losses to heat, and dissipated energy onto the vessel wall (see SI). Quantifying the specific energy, which is defined as the energy input per unit of reactant mass, is one puzzle piece to model reaction particle kinetics. Other non-trivial measurements, such as the mechanical behavior or stress–strain curve of a single particle crystal *via* nano-indentation, will be needed to develop a rigorous predictive framework for mechanochemical processes. Fig. 6C shows a significant decrease in specific kinetic energy as the fill ratio increases. In this single-ball vibratory mill, a lower fill ratio allows the ball to achieve higher velocities and undergo direct collisions with the vessel walls, thus imparting greater energy per unit mass. By contrast, a higher fill ratio, as shown in this figure, constrains the motion of the milling ball within the reactant mixture, leading to damping effects that absorb the kinetic energy before it can be effectively transmitted to the reactant. As more reactants occupy the vessel volume, the ball remains embedded in the mixture for a greater proportion of the milling cycle, resulting in a lower frequency of high-impact collisions and a broader dispersion of energy in the form of friction and heat. Consequently, the reduced impact efficiency translates into a lower net energy input for mechanochemical transformations. This observation is consistent with broader insights in ball milling, where optimal reaction parameters must be established to maximize

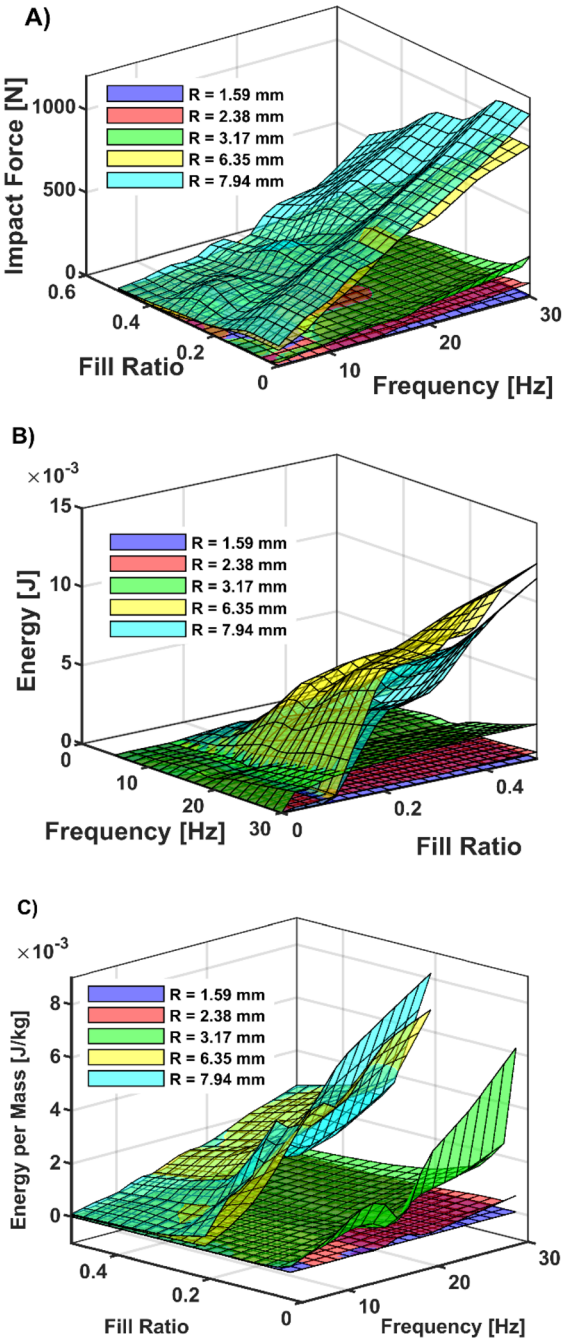

Fig. 6 (A) Measured impact force exerted by the milling ball onto the wall of the reactor jar. (B) Kinetic energy on reactant particles for different ball sizes with varying fill ratios. (C) Specific kinetic energy input on reactant mixture for different ball sizes with varying fill ratio.

collision intensity and ensure sufficient contact area for efficient mechanical activation.[46,47] The correlation between measured impact forces and mechanical activation energies shown in this study, while offering valuable quantitative insights into energy transfer mechanisms, requires careful evaluation of its applicability across various types of mechanochemical transformations. For the NaCl calibration system, the measured forces mainly reflect elastic and plastic

deformation processes in a crystalline ionic solid with well-defined mechanical properties. However, different classes of materials, such as organic molecular crystals, metal–organic frameworks, or polymer systems, display distinct mechanical responses to impact forces that may not directly correlate with the established force–energy relationships. The efficiency of various mechanochemical changes induced by mechanical treatment varies considerably. Therefore, while the force measurement approach offers a quantitative framework for energy analysis, the specific correlation factors should be considered material-specific rather than universal constants.

3.2. Kinetics simulation of an illustrative mechanochemical system to investigate the effect of the force ensemble seen in vibratory ball mills

In our previous work, we developed a framework to capture the effects of mechanical force on chemical kinetics during impact events in a ball mill reactor.[44] This approach uses transition state theory and continuum contact mechanics to show how force alters reaction rates. Here, the reaction rate constant as a function of the activation energy is reduced by mechanical energy

$$k(r,t) = A_0 \exp\left(-\frac{E_a - F\Delta x}{k_B T}\right), \quad (14)$$

where A_0 is the attempt frequency, E_a is the activation energy, F is the impact force, Δx is the effective path length along the reaction coordinate, k_B is a Boltzmann constant and T is the temperature. The pressure distribution within the contact described by the Hertz model is:

$$P(r,t) = \frac{3(F)}{2\pi a^2}\left(1 - \frac{r^2}{a^2}\right)^{1/2}, \quad (15)$$

where a is the contact radius. Next, the rate of change in reactant concentration within a contact becomes,

$$\frac{d\rho(r,t)}{dt} = A_0 \exp\left(-\frac{E_a - F\Delta x}{k_B T}\right)\rho(r,t)^n, \quad (16)$$

where $\rho(r,t)$ is the local reactant concentration. The modified total change in concentration after a single impact is given as

$$\Delta N = \int_0^a 2\pi h r \left(r_0 \exp\left(-\frac{E_a - F\Delta x}{k_B T}\right)\left(1 - \frac{r^2}{a^2}\right)^{\frac{1}{2}}\right) dr, \quad (17)$$

where h is the thickness of the reactant layer in the impact area.

In the present study, we evaluate the assumption that the mean impact force F yields the expected reaction rate as predicted by this model. To explore this, we numerically integrate eqn (17) using a Monte-Carlo approach, incorporating the experimentally measured force distribution of an illustrative mechanochemical reaction. This system was simulated using a stainless-steel ball and vessel (E = 210 GPa, ϖ = 0.29), with a total reaction mass of 2.5 g, ball radii between 1.59 and 7.93 mm, and reaction activation energy E_a = 0.7 eV. This reaction has a change in activation volume $\Delta V_a = 20$ Å^3 with temperature

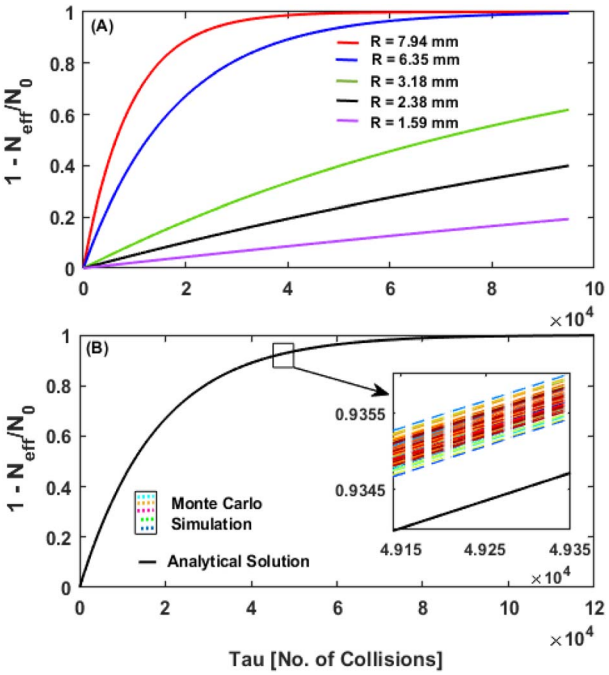

Fig. 7 Reaction kinetics using model. (A) Evolution of change in reactant concentration *versus* the number of collisions using various ball radii from 1.59 mm to 7.94 mm. (B) Zoomed-in kinetics comparison between analytical solution using mean impact force and effective kinetics using Monte Carlo simulation of force distribution around the mean impact force for ball radius R = 6.35 mm.

T = 300 K and an assumed value of attempt frequency $A_0 = 1 \times 10^{13}$ s^{-1}. The kinetic curves shown in Fig. 7 are obtained by varying ball sizes. Previously measured force ensembles (mean force and standard deviation) were used for each ball size. As shown in Fig. 7A, all curves behave exponentially for a first-order reaction. Kinetic curves for different ball sizes show how the reaction progresses for the force distribution centered on the mean impact force and known deviation. The normalized conversion $1 - N_{eff}/N_0$ increased with increasing ball size as larger balls tend to generate higher impact force, leading to more significant changes in the milled materials. The increased mechanical energy and contact surfaces in larger balls enhance particle–particle collision, accelerating the reaction. From the force model, the impact force is almost proportional to the square of the ball radius, and previous work on the energetics of collision between grinding media in ball mills detailed in the agreement how collision force, contact radius, time, and collision energy are all function of ball size as larger balls produce larger impact and are thus heavier at constant density suggesting heat generation effects on reactivity.[48] Variation in force distribution for a given ball radius and chosen ball mill setting produces a slight variation in reaction kinetics, thus creating a range under which reaction progression and kinetics are expected. This highlights the dynamic nature of mechanical impact in vibratory ball mills.

Fig. 7B shows that the kinetics of analytical solutions, which use mean impact force, are slightly slower than the Monte-Carlo (MC) simulation, which uses the force ensemble. Thus, the

mean impact force can be adequately used in kinetic modeling without concerns that the force ensemble applied to the reactant mixture will yield drastically different rates. Consequently, we extended the kinetic framework to assess the effect of the ball size and mass on this mechanochemical reaction system. By varying the ball size while maintaining the mass of the ball as opposed to Fig. 7A, where the ball size and mass were varied, the larger ball size led to a faster reaction rate, thus suggesting that the size of milling media plays an almost equal role in affecting kinetics as ball mass (see SI). This varying size effect is due to the larger balls activating more reactant powder per impact, thus enhancing the reaction rate, and agrees with previously conducted experimental studies.[49]

3.3. Kinetics as a function of fill ratio in the mechanochemical activation of Knoevenagel condensation reaction between vanillin and barbituric acid

Next, we vary the reactant vessel fill ratio in the Knoevenagel condensation reaction between vanillin and barbituric acid (Scheme 1) at 30 Hz for 60 minutes using a 12.7 mm ball diameter to provide insights into the influence of fill ratio on reaction conversion. Table 1 shows the reactant mixture with the vessel filled to 10%, 20%, 30%, 40%, and 50%.

Here, reaction conversions were 94% at both 10% and 20% fill ratio, 68% at 30% fill ratio, 19% at 40% fill ratio, and 26% at 50% fill ratio. These values are within typical uncertainties of ±5% due to experimental constraints. Reaction conversion remained high at lower fill ratios (10% and 20%) and decreased sharply from 30% to 50% (see SI). If the fill ratio were inconsequential, the conversion should scale with total mass, implying that conversion increases proportionally as the total mass increases. The total mass of reactants increases linearly with the fill ratio since ball volume and reactant vessel volume remain constant. Despite doubling the reactant mass, the conversion remains nearly constant from 10% to 20% fill ratio, suggesting that the total product scales linearly with mass and efficiency is maintained. However, beyond 20%, the conversion drops significantly, by approximately 27% to 68% at 30 percent fill, 80% to 19% at 40 percent fill, and then rises modestly to 26% at 50 percent fill. This behavior is consistent with our force model, which incorporates the fill ratio to assess its effect on impact force. The reduction factor, derived from experimental measurements (see SI), quantifies how the impact force reduces as the fill ratio increases. The observed drop in reaction conversion at higher fill ratios corresponds to energy saturation at the ball–reactant mixture interface. Beyond a certain threshold, particularly evident between 20% and 30% fill, additional reactant mass yields diminishing returns. Previous studies corroborate this phenomenon, demonstrating that densely packed beds primarily absorb rather than transmit applied forces.[50]

The observed saturation in conversion rates could be explained if the reactants in the impact behave like a liquid squeeze flow, where particles are freely displaced away from the impinging ball when the gap between the ball and the vessel is high, and only produce enough force to drive the reaction when the gap is sufficiently small.[51] Thus, increasing the reactants in the contact beyond this critical gap results in no significant increase in total energy transferred. Additionally, higher amounts of reactant particles begin to impede the motion of the ball and reduce the efficiency with which the shaking reactor vessel can impart new energy to the ball. The results presented in Table 1 then suggest that the optimum fill ratio for this reaction is ~20%, beyond which saturation and inefficient energy transfer occur.

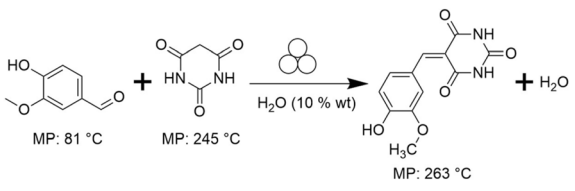

Scheme 1 The mechanochemical Knoevenagel condensation of vanillin and barbituric acid.

3.4. Experimental measurement of kinetic energy towards mechanical activation in the Knoevenagel condensation reaction between vanillin and barbituric acid

To quantitatively estimate the portion of energy going into the reactant mixture for mechanical activation, the Knoevenagel condensation reaction between vanillin and barbituric acid was carried out using the force-sensing vessels. Previous studies have shown that this reaction exhibits sigmoidal kinetics, characterized by an induction period followed by rapid product formation leading to completion. The acceleration in product formation after the induction period has been attributed to rheological changes within the reactant mixture, particularly at milling frequencies of 25 and 30 Hz using stainless steel milling media. These rheological changes, known as the "snowball effect," involve caking the reactant mixture around the milling ball after the induction period. With each impact, the caked layer grows, influencing the kinetics of the reaction as the "caked" ball would transmit less impact force to the reactants.[52–54] Another study shows this reaction proceeds through a cocrystal intermediate.[55] These studies suggest that rheology plays a role in the kinetics, especially in stainless steel milling media.

Here, we exploit the reported rheology change in the reactant mixture to quantify the impact forces and energy transfer during the reaction. The reaction was done with a total mass of 0.529 g (1.87 mmol of barbituric acid, 1.9 mmol of vanillin, and 3.26 mmol of water). Multiple trials were conducted using stainless steel milling vessels with grinding balls (12.7 mm diameter, 8.55 g mass), maintaining an estimated fill ratio of 10%. Experiments were performed at 15, 20, and 30 Hz milling frequencies to examine effects across various energies. Impact forces were recorded for 60-second intervals every 6 minutes during the reaction, enabling real-time tracking within the milling vessel. The mean impact forces and uncertainties were measured over the entire reaction time. At the onset of the reaction, the impact force indicated direct collisions between

Table 1 Reaction mixture for each fill ratio

Fill ratio (%)	Vanillin (mmol)	Barbituric acid (mmol)	Water (mmol)	Conversion (%)
10	0.87	0.87	1.33	94
20	5.83	5.83	8.89	94
30	10.79	10.79	16.44	68
40	15.74	15.74	24.00	19
50	20.70	20.70	31.56	26

the milling ball and the vessel wall, with a portion of the reactant mixture trapped between them at each impact. These forces aligned with expected values for unimpeded impacts. A notable finding is the pronounced dip in impact force observed during the middle part of the reaction. This decrease corresponds closely to a rheological transition from a predominantly crystalline reactant matrix (see SI) to a slurry-like mixture, which had been previously reported. By the end of the reaction, the measured impact force nearly matches that of an empty vessel, indicating that the milling ball no longer significantly interacts with a viscous medium. Instead, most of its kinetic energy is transferred directly to the vessel walls. It prompts further investigation into how the reactant mixture influences energy dissipation pathways, thereby shaping both the rate and the efficiency of mechanochemical transformations.

Fig. 8B shows the measured energy imparted to the reactant mixture, facilitating mechanical activation K_{act} as described in eqn (13). The reaction at 15 Hz for 180 minutes reached a reaction conversion of >71% with a measured energy input of 46.93 kJ mol^{-1}. Increasing the milling frequency to 20 Hz for 120 minutes improved the conversion to >77%, with energy input of 193.01 kJ mol^{-1}. Further increasing the frequency to 30 Hz for 60 minutes yielded over 86% product formation, increasing energy input to 283.3 kJ mol^{-1}. Extrapolating the data at 15 Hz to 100% conversion had an estimated energy of 66 kJ mol^{-1}, which falls within the range of solvothermal kinetics reported in the literature.[56] The excess energy input at higher milling frequencies tells us that only a fraction of the mechanical kinetic energy is effectively utilized to facilitate mechanical activation. Beyond the range of impact forces measured at 15 Hz, the increased impact force is directed into non-productive work, such as friction and heat generation, resulting in diminished overall reaction efficiency. This efficiency is calculated as,

$$\text{Efficiency} = \frac{\text{Mechanochemical work} \times \text{number of moles}}{\text{Total energy input}} \quad (18)$$

where mechanochemical work is the measured dissipated energy needed for the reactant mixture to undergo mechanical activation at 15 Hz. The total energy input is calculated as:

$$\text{Total energy input} = mv^2ft, \quad (19)$$

where m is the mass of the milling ball, v is the velocity, f is the frequency, and t is the time to reach the reaction conversion for each frequency. The reactor efficiency at 15 Hz is approximately 21.8%, dropping to 8.2% at 30 Hz – an approximate threefold decrease. Beyond the milling process, the overall system efficiency must account for the performance of key mechanical components, such as the brushless DC motor and mechanical bearings in these typical ball mill reactor systems. Studies show that brushless DC motors typically achieve efficiencies around 90% across their operating range, while mechanical bearings,

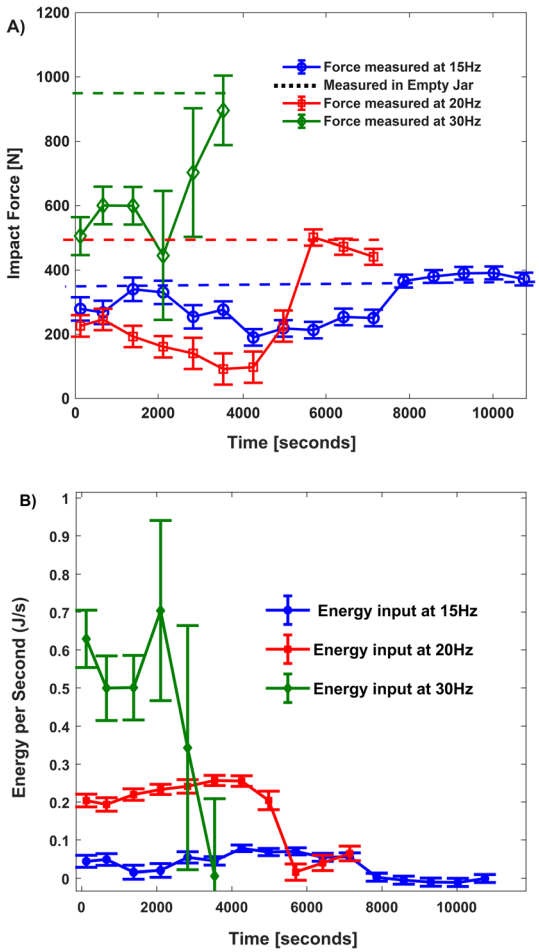

Fig. 8 Knoevenagel condensation reaction. (A) *In situ* measurement of mean impact force during the reaction using one 12.7 mm stainless steel ball in a stainless-steel jar at 15, 20, and 30 Hz. (B) Mean kinetic energy input on reactant particles towards mechanical activation at different frequencies. For Fig. 8A, mean uncertainty is used rather than the width of the force distribution since using the mean force yields the expected reaction rate (Fig. 7).

such as roller bearings, exhibit nearly 98%.[57–59] When these efficiencies are integrated into the energy chain—from electrical input to the motor, through the bearings, to the mechanical energy imparted to the milling ball—the overall system efficiency is notably lower than the milling process efficiency alone. Specifically, at 15 Hz, the combined system efficiency is approximately 19.2% and 7.23% at 30 Hz. This reduction reflects the cumulative effect of energy losses at each stage, emphasizing the need to consider the entire energy transfer pathway in mechanochemical systems. These findings highlight that the energetics of high-frequency milling may entail diminishing returns, reinforcing the idea that there can be an optimal balance between collision intensity, resulting impact forces, and productive energy usage. The force-sensing milling vessel employed in this study enabled the measurement of kinetic energy transferred to the reactants, allowing for the calculation of the dissipated energies required for mechanical activation. Such quantification is invaluable for guiding the scale-up of mechanochemical processes, as it reveals the frequencies and collisional forces that yield the highest product formation per unit energy input.

The Knoevenagel condensation reaction between vanillin and barbituric acid involves more complexity than just force–activation relationships. Due to vanillin's high volatility, the mechanochemical synthesis may not proceed solely through solid-state pathways as initially assumed.[60] Studies have shown that reactions involving volatile components can proceed through gas–solid or fluidized-state mechanisms, where the primary role of milling is to generate fresh particle surfaces that improve accessibility for molecules in gaseous or semi-liquid phases rather than applying direct mechanical activation energy.[55,61] In such systems, the relationship between impact force and reaction rate becomes more complex, as effectiveness depends not only on the energy transferred to break chemical bonds but also on the efficiency of surface generation, mixing, and mass transfer processes. The force measurements in this study mainly capture the energy associated with ball-vessel collisions and direct mechanical deformation; however, they may not fully account for the energy needed for thorough mixing of reactant phases, disruption of crystal lattices to expose reactive sites, or the formation of high-energy defect sites that enable molecular rearrangements. The rheological changes observed during the Knoevenagel reaction, described as the "snowball effect," suggest that the reaction involves complex phase transformations that go beyond simple mechanical activation. The efficiency of these mixing processes may not be directly proportional to the impact force, as gentle but consistent agitation can be more effective for specific reactions than high-energy impacts. These findings suggest that while force-sensing methods offer a valuable tool for understanding energy transfer in mechanochemical systems, each reaction necessitates specific calibration and validation to establish meaningful relationships between force and activation. The reaction efficiencies observed for the Knoevenagel system should be viewed as particular to this reaction under the tested conditions, rather than as a universal standard. Future studies should systematically examine how material properties, reaction mechanisms, and physical states influence the force–activation relationship.

Despite these limitations, the force-sensing methodology developed in this study provides an essential foundation for rational mechanochemical reactor design. The quantitative understanding of energy partitioning, even if system-specific, enables more informed optimization of milling parameters and offers insights into the limits of reaction efficiency. The framework established here marks a significant step toward predictive mechanochemistry, where reactor parameters can be optimized based on quantitative energy analysis rather than empirical trial-and-error methods. Nevertheless, the successful application of this methodology to new systems will require careful consideration of the specific material properties, reaction mechanisms, and activation pathways involved, along with appropriate calibration studies for each new class of mechanochemical transformations.

4. Conclusions

By embedding piezoresistive sensors directly into the reactor jar of a vibratory ball mill, we take an initial step toward quantifying the impact forces and energy for mechanical activation. The resulting force ensemble is a time-resolved distribution of primary and secondary impacts that aligns with an adjusted Hertzian-based force model, which predicts impact forces across a wide range of operational settings. We find that the impact of milling media on the reactants acts as an ensemble of forces applied dynamically. Notably, kinetics simulations revealed that employing the force ensemble produced reaction kinetics similar to those obtained using the mean impact force, with a slight difference. We demonstrated energy quantification toward mechanical activation by exploiting the rheological changes within the reactant mixture in the Knoevenagel condensation reaction. For this mechanochemical system and reactor type, the collision amplitude increases quadratically with frequency; however, the energy-transfer efficiency decreases from 22% at 15 Hz to 8% at 30 Hz, as non-productive energy pathways become dominant. Ball diameter exerts a $F \propto R^2$ dependence and activates more powder per hit, but its net kinetic benefit mirrors that of simply adding mass, reflecting classic energy-yield observations. Powder loading proves far more sensitive, with performance peaking at about 20% fill, while a 50% fill reduces impact force by 70% through ball confinement and particle damping. We also demonstrate that high-frequency milling in vibratory ball mills involves a trade-off, where increasing collision intensity and impact forces eventually lead to diminishing returns, suggesting an optimal balance for efficient energy use. Collectively, these insights provide a practical guide: optimize the fill ratio first, tune the ball mass or size second, and increase the frequency only until marginal gains are achieved for effective energy transfer in mechanochemical systems. Importantly, we emphasize that these efforts should not yet be regarded as universally applicable to every mill or reaction type, as they represent progressive steps toward generalizing force-resolved reactor design across the diverse landscape of mechanochemical transformations.

Author contributions

Author contributions to this work according to CRediT standardized contribution descriptions are as follows: EN (conceptualization, data curation, formal analysis, investigation, methodology, visualization, writing), KF (investigation, writing – review, and editing), JF (conceptualization, project administration, visualization, supervision, writing), and JB (conceptualization, funding acquisition, project administration, resources, supervision, writing).

Conflicts of interest

There are no conflicts to declare.

Note added after first publication

This article replaces the version published on 19th September 2025. The title for column 5 of Table 1 has been updated and column 6 has been removed.

Data availability

Raw files have been deposited at the repository with the link: **https://doi.org/10.6084/m9.figshare.28899125**.

Data supporting this article have been included in the Supporting Information (SI). See DOI: **https://doi.org/10.1039/d5mr00059a**.

Acknowledgements

This work was supported by the NSF Center for the Mechanical Control of Chemistry under grant no. CHE-2303044.

Notes and references

1 P. Baláž, M. Achimovičová, M. Baláž, P. Billik, Z. Cherkezova-Zheleva, J. M. Criado, F. Delogu, E. Dutková, E. Gaffet, F. J. Gotor, R. Kumar, I. Mitov, T. Rojac, M. Senna, A. Streletskii and K. Wieczorek-Ciurowa, *Chem. Soc. Rev.*, 2013, **42**, 7571–7637.
2 E. Y. Shalaev and G. Zografi, *J. Phys. Org. Chem.*, 1996, **9**, 729–738.
3 J.-L. Do and T. Friščić, *ACS Cent. Sci.*, 2017, **3**, 13–19.
4 A. A. Michalchuk, E. V. Boldyreva, A. M. Belenguer, F. Emmerling and V. V. Boldyrev, *Front. Chem.*, 2021, **9**, 685789.
5 V. V. Boldyrev, *Russ. Chem. Rev.*, 2006, **75**, 177.
6 V. Martinez, T. Stolar, B. Karadeniz, I. Brekalo and K. Užarević, *Nat. Rev. Chem.*, 2023, **7**, 51–65.
7 S. Pagola, *Crystals*, 2023, **13**, 124.
8 E. Ivanov and C. Suryanarayana, *J. Mater. Synth. Process.*, 2000, **8**, 235–244.
9 M. K. Beyer and H. Clausen-Schaumann, *Chem. Rev.*, 2005, **105**, 2921–2948.
10 K. R. Rajaonarivony, C. Mayer-Laigle, B. Piriou and X. Rouau, *Energy*, 2021, **227**, 120508.
11 L. Y. Sadler III, D. A. Stanley and D. R. Brooks, *Powder Technol.*, 1975, **12**, 19–28.
12 L. Vugrin, M. Carta, S. Lukin, E. Meštrović, F. Delogu and I. Halasz, *Faraday Discuss.*, 2023, **241**, 217–229.
13 A. H. Hergesell, C. L. Seitzinger, J. Burg, R. J. Baarslag and I. Vollmer, *RSC Mechanochem.*, 2025, **2**, 263–272.
14 S. Hwang, S. Grätz and L. Borchardt, *Chem. Commun.*, 2022, **58**, 1661–1671.
15 R. A. Hernandez R, N. Nabavi, S. J. Patterson and P. Forgione, *ChemCatChem*, 2024, **16**, e202400406.
16 P. Chattopadhyay, I. Manna, S. Talapatra and S. Pabi, *Mater. Chem. Phys.*, 2001, **68**, 85–94.
17 Y. Altıntas and P. Lee, *J. Manuf. Sci. Eng.*, 1998, **120**, 684–692.
18 A. M. Belenguer, G. I. Lampronti and J. K. Sanders, *Isr. J. Chem.*, 2021, **61**, 764–773.
19 A. Yazdani, M. Hadianfard and E. Salahinejad, *J. Alloys Compd.*, 2013, **555**, 108–111.
20 H. Huang, J. Pan and P. McCormick, *Mater. Sci. Eng., A*, 1997, **232**, 55–62.
21 V. Buchholtz, J. A. Freund and T. Pöschel, *Eur. Phys. J. B*, 2000, **16**, 169–182.
22 M. Mhadhbi, *Adv. Mater. Phys. Chem.*, 2021, **11**, 31–44.
23 M. Carta, F. Delogu and A. Porcheddu, *Phys. Chem. Chem. Phys.*, 2021, **23**, 14178–14194.
24 M. Bab and L. Mendoza-Zélis, *Scr. Mater.*, 2004, **50**, 99–104.
25 G. Cagnetta, J. Huang, B. Wang, S. Deng and G. Yu, *Chem. Eng. J.*, 2016, **291**, 30–38.
26 E. G. Avvakumov, M. Senna and N. Kosova, *Soft Mechanochemical Synthesis: A Basis for New Chemical Technologies*, Springer Science & Business Media, 2001.
27 F. Urakaev, in *High-Energy Ball Milling*, Elsevier, 2010, pp. 9–44.
28 V. Smolyakov, O. Lapshin and V. Boldyrev, *Theor. Found. Chem. Eng.*, 2008, **42**, 54–59.
29 T. Yusupov, L. Shumskaya, S. Kondrat'ev, E. Kirillova and F. K. Urakaev, *J. Min. Sci.*, 2019, **55**, 804–810.
30 P. Y. Butyagin and I. Pavlichev, *React. Solids*, 1986, **1**, 361–372.
31 P. Y. Butyagin and A. Streletskii, *Phys. Solid State*, 2005, **47**, 856–862.
32 A. S. Rogachev, *Russ. Chem. Rev.*, 2019, **88**, 875.
33 W. Wang, PhD thesis, The University of Waikato, 2000.
34 D. R. Maurice and T. Courtney, *Metall. Trans. A*, 1990, **21**, 289–303.
35 F. K. Urakaev and V. Boldyrev, *Powder Technol.*, 2000, **107**, 93–107.
36 D. Maurice and T. Courtney, *Metall. Mater. Trans. A*, 1996, **27**, 1973–1979.
37 R. Watanabe, H. Hashimoto and G. G. Lee, *Mater. Trans., JIM*, 1995, **36**, 102–109.
38 M. Kessler and R. Rinaldi, *Front. Chem.*, 2022, **9**, 816553.
39 W. Schmidt, P. Losch, H. Petersen, M. Etter, F. Baum, J. Ternieden and C. Weidenthaler, *RSC Mechanochem.*, 2025, **2**, 273–284.
40 M. Carta, L. Vugrin, G. Miletić, M. J. Kulcsár, P. C. Ricci, I. Halasz and F. Delogu, *Angew. Chem., Int. Ed.*, 2023, **62**, e202308046.

41 F. Delogu and L. Takacs, *Acta Mater.*, 2014, **80**, 435–444.
42 F. Delogu and L. Takacs, *J. Mater. Sci.*, 2018, **53**, 13331–13342.
43 C. Qu, L. Fang and R. W. Carpick, *Phys. Rev. B*, 2025, **111**, 195405.
44 E. Nwoye, S. Raghuraman, M. Costales, J. Batteas and J. R. Felts, *Phys. Chem. Chem. Phys.*, 2023, **25**, 29088–29097.
45 S. S. Razavi-Tousi and J. A. Szpunar, *Powder Technol.*, 2015, **284**, 149–158.
46 M. Kessler and R. Rinaldi, *Front. Chem.*, 2022, **9**, 816553.
47 H. Shin, S. Lee, H. Suk Jung and J.-B. Kim, *Ceram. Int.*, 2013, **39**, 8963–8968.
48 K. S. Venkataraman and K. S. Narayanan, *Powder Technol.*, 1998, **96**, 190–201.
49 A. A. L. Michalchuk, I. A. Tumanov and E. V. Boldyreva, *CrystEngComm*, 2019, **21**, 2174–2179.
50 A.-S. Persson and G. Frenning, *Powder Technol.*, 2012, **219**, 249–256.
51 J. Engmann, C. Servais and A. S. Burbidge, *J. Non-Newtonian Fluid Mech.*, 2005, **132**, 1–27.
52 C. F. Burmeister, R. Schmidt, K. Jacob, S. Breitung-Faes, A. Stolle and A. Kwade, *Chem. Eng. J.*, 2020, **396**, 124578.
53 M. Carta, S. L. James and F. Delogu, *Molecules*, 2019, **24**, 3600.
54 B. P. Hutchings, D. E. Crawford, L. Gao, P. Hu and S. L. James, *Angew. Chem., Int. Ed.*, 2017, **56**, 15252–15256.
55 S. Lukin, M. Tireli, I. Lončarić, D. Barišić, P. Šket, D. Vrsaljko, M. di Michiel, J. Plavec, K. Užarević and I. Halasz, *Chem. Commun.*, 2018, **54**, 13216–13219.
56 R. Behjatmanesh-Ardakani, N. Safaeian, M. Oftadeh and M. Fallah-Mehrjardi, *Theor. Chem. Acc.*, 2020, **139**, 45.
57 M. Miyamasu and K. Akatsu, *IEEJ J. Ind. Appl.*, 2013, **2**, 79–86.
58 T.-H. Hsieh, S. H. Yeon and H. Herr, *Actuators*, 2023, **12**, 318.
59 N. Bratu-Serban, E. Guzmán-Serrano, J. Rodríguez, R. Morales, *Univ. Power Eng. Conf.* 2001.
60 A. R. Almeida, V. L. Freitas, J. I. Campos, M. D. R. da Silva and M. J. Monte, *J. Chem. Thermodyn.*, 2019, **128**, 45–54.
61 M. J. Cliffe, C. Mottillo, R. S. Stein, D.-K. Bučar and T. Friščić, *Chem. Sci.*, 2012, **3**, 2495–2500.